Journal of ELECTRONIC MATERIALS, Vol. 47, No. 4, 2018
https://doi.org/10.1007/s11664-018-6067-2
© 2018 The Minerals, Metals & Materials Society

Intermetallic Compound Growth between Electroless Nickel/Electroless Palladium/Immersion Gold Surface Finish and Sn-3.5Ag or Sn-3.0Ag-0.5Cu Solder

YUKINORI ODA,[1,2] NAOKI FUKUMURO,[1] and SHINJI YAE[1,3]

1.—Department of Chemical Engineering and Materials Science, Graduate School of Engineering, University of Hyogo, Himeji, Hyogo 671-2280, Japan. 2.—Central Research Laboratory, C. Uyemura & Co., Ltd., Hirakata, Osaka 573-0065, Japan. 3.—e-mail: yae@eng.u-hyogo.ac.jp

Using an electroless nickel/electroless palladium/immersion gold (ENEPIG) surface finish with a thick palladium–phosphorus (Pd-P) layer of 1 μm, the intermetallic compound (IMC) growth between the ENEPIG surface finish and lead-free solders Sn-3.5Ag (SA) or Sn-3.0Ag-0.5Cu (SAC) after reflow soldering and during solid-state aging at 150°C was investigated. After reflow soldering, in the SA/ENEPIG and SAC/ENEPIG interfaces, thick $PdSn_4$ layers of about 2 μm to 3 μm formed on the residual Pd-P layers ($\sim$ 0.5 μm thick). On the SA/ENEPIG interface, Sn was detected on the upper side of the residual Pd-P layer. On the SAC/ENEPIG interface, no Sn was detected in the residual Pd-P layer, and Cu was detected in the interface between the Pd-P and $PdSn_4$ layers. After 300 h of aging at 150°C, the residual Pd-P layers had diffused completely into the solders. In the SA/ENEPIG interface, an IMC layer consisting of Ni_3Sn_4 and Ni_3SnP formed between the $PdSn_4$ layer and the nickel–phosphorus (Ni-P) layer, and a $(Pd,Ni)Sn_4$ layer formed on the lower side of the $PdSn_4$ layer. On the SAC/ENEPIG interface, a much thinner $(Pd,Ni)Sn_4$ layer was observed, and a $(Cu,Ni)_6Sn_5$ layer was observed between the $PdSn_4$ and Ni-P layers. These results indicate that Ni diffusion from the Ni-P layer to the $PdSn_4$ layer produced a thick $(Pd,Ni)Sn_4$ layer in the SA solder case, but was prevented by formation of $(Cu,Ni)_6Sn_5$ in the SAC solder case. This causes the difference in solder joint reliability between SA/ENEPIG and SAC/ENEPIG interfaces in common, thin Pd-P layer cases.

Key words: Lead-free solder, ENEPIG, solid-state aging, interfacial microstructure, diffusion barrier

INTRODUCTION

As electronic components have become smaller and lighter, surface mounting has become the mainstream approach for their packaging. Substrate wiring has also been developed for fine patterns. Thus, their surface finish has been changed to an electroless nickel/immersion gold (ENIG) process from the electrolysis Ni/Au process. On the other hand, since lead-containing eutectic solders have been regulated by governments in response to environmental movements, lead-free solders have become commonly used and electroless nickel/electroless palladium/immersion gold (ENEPIG) surface finish is superseding ENIG, because the mounting temperature for lead-free solders is higher than that for eutectic lead solders. ENEPIG surface finish is suitable not only for lead-free soldering but also for wire bonding.[1]

$PdSn_4$, which is an alloy that is easily formed between Pd and Sn, resembles fragile $AuSn_4$.[2–4] Regarding the solder joint characteristics of ENEPIG, both Sn-3.5Ag (in wt.%, SA) and Sn-3.5Ag-0.5Cu (in wt.%, SAC) exhibit satisfactory

(Received August 12, 2017; accepted January 4, 2018; published online January 12, 2018)

characteristics immediately after reflow soldering. However, the solder joint characteristics change after long-term thermal aging at 150°C; the characteristics for SA solder degrade and became unsatisfactory for use, while the characteristics are retained for SAC solder.[1] According to previous analysis of intermetallic compounds (IMCs), Ni_3Sn_4 and $(Pd,Ni)Sn_4$ were formed in the SA/ENEPIG interface, while $(Cu,Ni)_6Sn_5$ IMC formed in the SAC/ENEPIG interface on aging.[1,5,6] $(Au,Ni)Sn_4$ alloy, which resembles $(Pd,Ni)Sn_4$ alloy, was redeposited on the Ni_3Sn_4 IMC in a solder/ENIG interface after heat treatment.[7] Therefore, the mechanism of IMC growth in lead-free solder/ENEPIG interfaces is assumed to be the same as that in the Au case. When a $(Pd,Ni)Sn_4$ layer forms on the Ni_3Sn_4 layer, the characteristics of the solder joint deteriorate.[1] The influence of the Pd concentration on the reaction between Ni and Sn-xPd alloys (where x = 0 wt.% to 1 wt.%) in SAC solder at 250°C was examined by Ho et al.[8] They indicated that, when the Pd concentration reaches 0.3 wt.%, an additional compound, viz. $(Pd,Ni)Sn_4$, appeared, and the high-speed ball shear test resistance started to decay, indicating that presence of $(Pd,Ni)Sn_4$ would degrade the mechanical reliability of the joint interface.[8] To prevent such degradation, it is important to determine the formation mechanism of such a $(Pd,Ni)Sn_4$ layer that originates from $PdSn_4$ formed by reflow soldering of ENEPIG surface finish. $PdSn_4$ IMC is formed in both SA and SAC solders with thick Pd layers.[9] Presence of $(Pd,Ni)Sn_4$ would degrade the mechanical reliability of the joint interface.[10,11] However, its formation mechanism remains to be clarified. In this study, with a thick (1 μm) palladium–phosphorus (Pd-P) layer, the growth mechanism of the $(Pd,Ni)Sn_4$ IMC layer between ENEPIG surface finish and lead-free solder Sn-3.5Ag (SA), and the preventive mechanism of such IMC growth in the case of Sn-3.0Ag-0.5Cu (SAC), were investigated after reflow soldering and during solid-state aging at 150°C.

EXPERIMENTAL PROCEDURES

The test substrates used were copper-clad laminate coupons to which 20-μm-thick electrolytic copper was plated. For one of them, a 0.5-mm-diameter ball grid array pattern was developed using a solder mask. Table I shows the process and conditions used for the ENEPIG surface finish. For plating, we used commercially available plating chemicals manufactured by C. Uyemura & Co., ltd. The thicknesses of the nickel–phosphorus (Ni-P), palladium–phosphorus (Pd-P), and Au layers were adjusted to 5 μm, 1 μm, and 0.06 μm, respectively, by changing the plating time. The phosphorus concentration of Ni-P was about 6 wt.% to 8 wt.%, while that of Pd-P was about 5 wt.% to 6 wt.%. The thickness of each layer was measured by x-ray fluorescence analysis thickness meter (Fischer XDV-μ). Sn-3.5Ag solder (in wt.%, SA, Senju Metal Industry M30) or Sn-3.5Ag-0.5Cu solder (in wt.%, SAC, Senju Metal Industry M705) was mounted with flux (Senju Metal Industry Delta flux 529D-1) on ENEPIG-surface-finished substrate, and reflow soldering was performed under air atmosphere with maximum temperature of 240°C for 35 s. After reflow soldering, solid-state aging was performed under air atmosphere at 150°C for 300 h, 700 h, and 1000 h. The interfacial structure of the solder joints was observed by field-emission scanning electron microscopy (FE-SEM, Zeiss ULTRA55), and the composition of each layer was analyzed by energy-dispersive x-ray spectroscopy (EDS, EDAX). Cross-sections of the soldered and aged joints were prepared using a cross-section polisher (JEOL SM-0910). The crystal structure of the IMCs formed in the substrate after aging was analyzed by x-ray diffraction (XRD, Rigaku SmartLab). We also analyzed the microstructure of the IMC formed after reflow soldering by transmission electron microscopy (TEM, JEOL JEM-2100). The TEM samples were prepared using an ultramicrotome (Leica Ultracut UCT) and a focused ion beam system (FIB, SII Xvision 200 DB).

RESULTS AND DISCUSSION

The results of the cross-sectional observations of the interfacial microstructure just after reflow soldering using SA and SAC solders are shown in Fig. 1a and b, respectively. In the SA solder case, thick $PdSn_4$ layers of about 2 μm to 3 μm formed between the residual Pd-P layers ($\sim$ 0.5 μm) and solder. In the SAC solder case, the cross-sectional structure resembled that of the SA solder. The Pd-P layer remained approximately half of the original deposit. A thick $PdSn_4$ layer was formed between the Pd-P layer and the solder for both solder materials. Cross-sectional SEM images and concentration profiles obtained by EDS line scans of the solder joint interface after reflow soldering using SA and SAC solders are shown in Fig. 2a and b, respectively. In the SA solder case, because high concentrations of Sn and P were detected in the upper part of the Pd-P layer (Fig. 2a and b), the $PdSn_4$ and Pd-Sn-P layers were probably formed due to interdiffusion between the solder and Pd-P layer. For the SAC solder, Sn was not detected in the Pd-P layer, however trace Cu was detected between the Pd-P and $PdSn_4$ layers (Fig. 2c and d). These results suggest that the Cu contained in the SAC solder segregated as Cu_6Sn_5 IMC on the Pd-P layer. Figure 3 shows the results of cross-sectional TEM analysis of the thick Pd-Sn IMC ($PdSn_4$) layer that formed on the SA/ENEPIG interface. We clarified that most of the Pd-Sn IMC layer consisted of $PdSn_4$ from the lattice image and the diffraction spot corresponding to the $PdSn_4$(100), (120), and (020) planes in the selected-area electron diffraction (SAED) patterns (Fig. 3a–c). A reflection

corresponding to the $PdSn_3$ (002) plane was also observed in the SAED pattern obtained from the lower side of the Pd-Sn IMC layer (Fig. 3d).

After reflow soldering, solid-state aging at 150°C under air atmosphere for 300 h was performed. The results of cross-sectional SEM observations and EDS line analysis for the SA/ENEPIG and SAC/ENEPIG interfaces are shown in Fig. 4. The Pd-P layers in both solder samples were completely diffused into the solder, and the $PdSn_4$ layer became thick concurrently, and new IMC layers approximately 0.5 μm thick and P-rich layers were observed between the $PdSn_4$ and Ni-P layers. In the SA solder case, a Ni-Sn-P layer was formed due to interdiffusion between the Ni-P and $PdSn_4$ layers (Fig. 4a and b). A thin Ni-Sn-P layer of approximately 0.1 μm is generally formed when soldering with ENIG surface finish.[7,12–14] In this study, the Ni-Sn-P layer thickened to approximately 1 μm because we used a thick Pd-P layer. We confirmed that two kinds of component existed in the Ni-Sn-P layer: high and low phosphorus concentration phases. Ni also diffused into the $PdSn_4$ layer, as confirmed by EDS line analysis (Fig. 4b).[15] On the other hand, on the SAC/ENEPIG interface, between $PdSn_4$ and Ni-P layers, a new IMC layer containing high concentrations of Cu, Ni, and Sn was identified as $(Cu,Ni)_6Sn_5$ (Fig. 4c and d).[1,14]

Figure 5 shows the results of cross-sectional SEM observations and EDS analysis for the solder/ENEPIG interfaces after aging at 150°C for 1000 h. Compared with the results for 300 h of aging at 150°C (Fig. 4), the only difference is that all

Table I. Process and conditions for ENEPIG surface finish

Process	Product name	Temp.	Time
Cleaner	ACL-009	50°C	5 min
Rinse			
Soft etching	SPS type	25°C	2 min
Rinse			
Acid rinse	10% H_2SO_4	R.t.	1 min
Rinse			
Pre-dipping	3% H_2SO_4	R.t.	1 min
Activator	MNK-4	30°C	2 min
Rinse			
Electroless Ni-P	NPR-4	80°C	30 min
Rinse			
Electroless Pd-P	TPD-30	50°C	90 min
Rinse			
Immersion Au	TSB-72	82°C	12 min

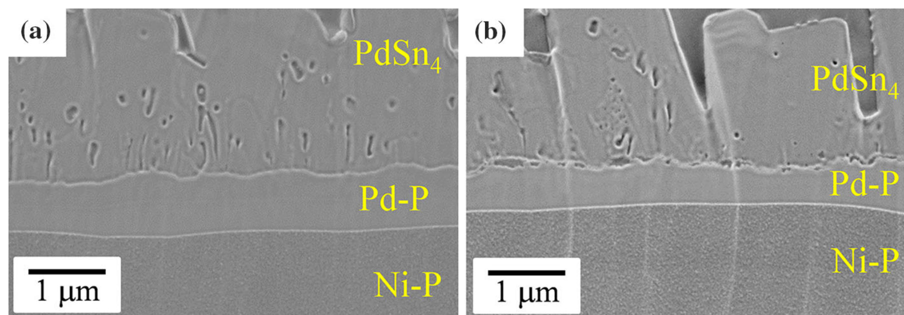

Fig. 1. Cross-sectional SEM images of solder joint interfaces after reflow soldering using (a) SA and (b) SAC solder.

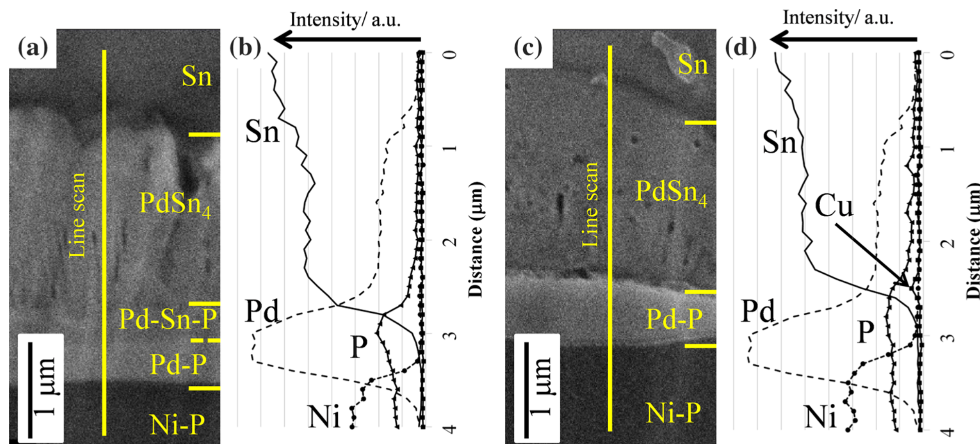

Fig. 2. Cross-sectional SEM images of solder joint interface after reflow soldering using (a) SA and (b) SAC solder. Concentration profiles from EDS line scans of (a) and (c) are shown in (b) and (d).

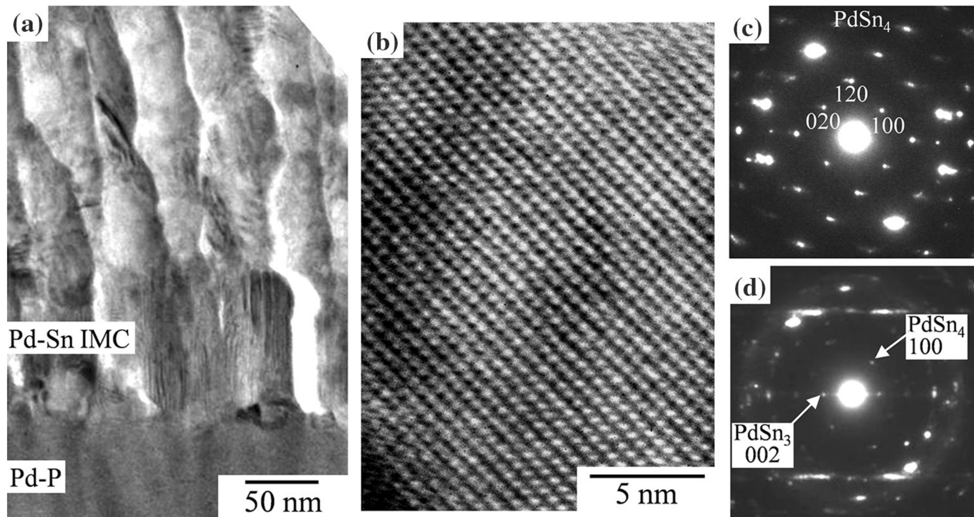

Fig. 3. Cross-sectional TEM images and selected-area electron diffraction (SAED) patterns of Pd-Sn IMC layer using SA solder after reflow soldering: (a) Pd-Sn IMC/Pd-P interface, (b) magnified image of Pd-Sn IMC, (c) SAED pattern of upper side of Pd-Sn IMC layer, and (d) SAED pattern of lower side of Pd-Sn IMC layer.

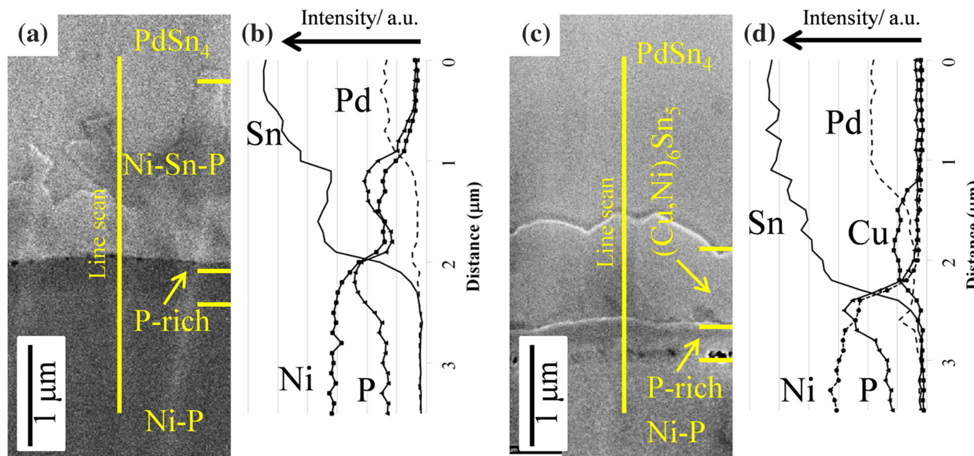

Fig. 4. Cross-sectional SEM images of SA/ENEPIG (a) and SAC/ENEPIG (b) interfaces after solid-state aging at 150°C for 300 h. Concentration profiles from EDS line scans of (a) and (c) are shown in (b) and (d).

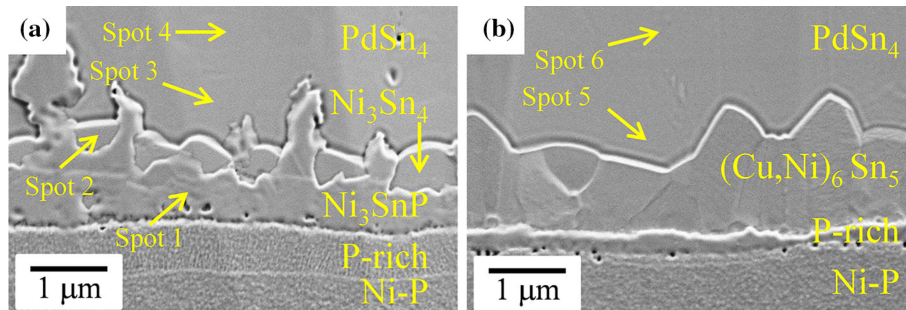

Fig. 5. Cross-sectional SEM images of SA/ENEPIG (a) and SAC/ENEPIG (b) interfaces after solid-state aging at 150°C for 1000 h.

the IMC layers were slightly thicker. To confirm the structure of the two kinds of IMCs formed in the SA solder, EDS spot analysis was performed. The phosphorus concentration exceeded 10 at.% for spot 1 and approximately 3 at.% for spot 2 (Fig. 5a). From the XRD analysis results, many kinds of IMCs

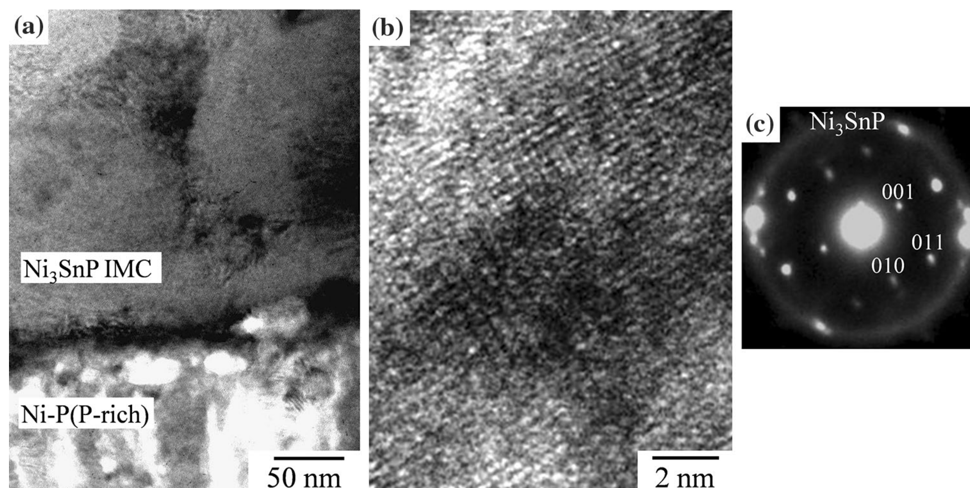

Fig. 6. Cross-sectional TEM images and selected-area electron diffraction (SAED) patterns of Ni_3SnP IMC layer after solid-state aging at 150°C for 1000 h: (a) Ni_3SnP IMC/Ni-P interface, (b) magnified image of Ni_3SnP IMC, and (c) SAED pattern of Ni_3SnP IMC layer.

(Ni_3Sn_4, Ni_3SnP, $PdSn_4$, Ag_3Sn, and β-Sn) were identified. Figure 6 shows the results of cross-sectional TEM analysis of the P-rich layer of Ni-P and the Ni-Sn-P layer formed in the SA/ENEPIG interface. Diffraction spots corresponding to Ni_3SnP (001), (010), and (011) planes were identified (Fig. 6-a–c). Spot 1 was ascribed to the Ni_3SnP phase, and spot 2 was ascribed to the Ni_3Sn_4 phase. Since P diffusion from the Ni-P layer to the solder side does not occur during solid-state aging,[7] the Ni_3SnP layer was formed by Sn diffusion from the $PdSn_4$ layer. Since the Ni diffused to the $PdSn_4$ layer, the Ni concentration of spots 3 and 4 was 14.6 at.% and 9.6 at.%, respectively. We previously reported that $(Pd,Ni)Sn_4$ phase was formed in the SA/ENEPIG interface with a thin (0.05 μm) Pd-P layer after aging at 150°C for 1000 h.[1] Therefore, we revealed that the $(Pd,Ni)Sn_4$ layer was formed by Ni diffusion from Ni_3Sn_4 and/or Ni_3SnP to the $PdSn_4$ layer. In the SAC solder case, the $(Cu,Ni)_6Sn_5$ layer was observed to be identical under the 300-h-aging condition (Fig. 4c). The Ni concentration of spots 5 and 6 (Fig. 5b) in the $PdSn_4$ layer was uniform and lower than that at spots 3 and 4 (Fig. 5a), viz. approximately 5 at.%. These results reveal that Ni diffusion did not proceed from the $(Cu,Ni)_6Sn_5$ layer to the $PdSn_4$ layer during solid-state aging.

CONCLUSIONS

Using a thick Pd-P layer, the growth mechanism of the $(Pd,Ni)Sn_4$ IMC layer, which reduces solder joint reliability, between the ENEPIG surface finish and SA solder, and the preventive mechanism of such IMC growth in the case of SAC solder, were investigated. Analysis of the change in the interfacial microstructure in the ENEPIG surface finish with a 1-μm-thick Pd-P layer during solid-state aging at 150°C after reflow soldering clearly revealed differences in IMC growth between the Sn-3.5Ag (SA) and Sn-3.0Ag-0.5Cu (SAC) solders. In the SA solder case, Ni_3SnP and Ni_3Sn_4 layers formed, then a $(Pd,Ni)Sn_4$ layer formed as Ni diffusion from the Ni-P layer proceeded. On the other hand, in the SAC solder case, we revealed that Ni diffusion from the Ni-P layer to the $PdSn_4$ layer was prevented by formation of $(Cu,Ni)_6Sn_5$. These results for a thick Pd-P layer indicate that Ni diffusion to SA solder and prevention of such diffusion by a $(Cu,Ni)_6Sn_5$ layer cause the difference in solder joint reliability between SA/ENEPIG and SAC/ENEPIG interfaces in common, thin Pd-P layer cases.

REFERENCES

1. Y. Oda, M. Kiso, S. Kurosaka, A. Okada, K. Kitajima, and S. Hashimoto, in *Proceeding of International Microelectronics and Packaging Society, IMAPS* (2008).
2. W.H. Wu, C.S. Lin, S.H. Huang, and C.E. Ho, *J. Electron. Mater.* 38, 2387 (2010).
3. S. Nakahara and R.J. McCoy, *Thin Solid Films* 88, 285 (1982).
4. G. Sharma, C.M. Eichfeld, and S.E. Mohney, *J. Electron. Mater.* 32, 1209 (2003).
5. Y.M. Kim, J.Y. Park, and Y.H. Kim, *J. Electron. Mater.* 41, 763 (2012).
6. K. Masui and M. Kajihara, *J. Alloys Compd.* 485, 144 (2009).
7. V. Vuorinen, T. Laurila, H. Yu, and J.K. Kivilahti, *J. Appl. Phys.* 99, 3530 (2006).
8. C.E. Ho, L.H. Hsu, S.W. Lin, and M.A. Rahman, *J. Electron. Mater.* 41, 2 (2012).
9. C.P. Lin and C.M. Chen, *J. Alloys Compd.* 547, 37 (2013).
10. C.E. Ho, T.T. Kuo, C.C. Wang, and W.H. Wu, *Electron. Mater. Lett.* 8, 495 (2012).
11. C.E. Ho, W.Z. Hsieh, C.H. Yang, T.C. Yeh, and T.T. Kuo, *J. Electron. Mater.* 44, 568 (2015).
12. D.G. Kim and S.B. Jung, *Mater. Trans.* 46, 1295 (2005).
13. C.C. Chi and T.H. Chuang, *J. Electron. Mater.* 35, 471 (2006).
14. C.W. Hwang, M. Kiso, S. Hashimoto, and K. Suganuma, *J. Mater. Res.* 18, 2540 (2003).
15. M.A. Rahman, C.E. Ho, W. Gierlotka, and J.C. Kuo, *J. Electron. Mater.* 43, 4582 (2014).